ACS Sustainable Chemistry & Engineering

Research Article

pubs.acs.org/journal/ascecg

Green, Noncorrosive, Easy Scale-Up Hydrothermal–Thermal Conversion: A Feasible Solution to Mass Production of Magnesium Borate Nanowhiskers

Wancheng Zhu,*[,†] Ruguo Wang,[†] Shanlin Zhu,[†] Linlin Zhang,[†] Xili Cui,[†] Heng Zhang,[†] Xianglan Piao,[‡] and Qiang Zhang*[,‡]

[†]Department of Chemical Engineering, Qufu Normal University, Shandong 273165, China

[‡]Department of Chemical Engineering, Tsinghua University, Beijing 100084, China

Supporting Information

ABSTRACT: Wet chemistry-based techniques, including widely used hydrothermal and solvothermal synthesis, have emerged as thriving strategies for nanostructure bulk synthesis, which in reality encountered the ubiquitous challenge of corrosion problems during scale-up or further commercialization. In this contribution, as an endeavor, uniform and pore-free $Mg_2B_2O_5$ nanowhiskers with a length of 120–3000 nm, a diameter of 40–160 nm, and an aspect ratio of 2–34 were successfully synthesized via a novel, green, noncorrosive, easy scale-up hydrothermal–thermal conversion route. Specifically, the NaCl byproduct of the room-temperature coprecipitation system was preseparated by filtration, and then the cake was transferred for hydrothermal conversion to avoid the corrosion of Cl^-, giving rise to uniform $MgBO_2(OH)$ nanowhiskers. The $MgBO_2(OH)$ nanowhiskers were calcined for high crystallinity $Mg_2B_2O_5$ nanowhiskers, assisted by NP-9 and preseparated byproduct NaCl. The present novel hydrothermal synthetic route to $MgBO_2(OH)$ nanowhiskers was carried out at 200 °C (40 °C lower than previous work), definitely indicating green characteristics, such as energy savings, reduction and reuse of byproduct, noncorrosiveness to hydrothermal apparatus, and easy scale-up. The as-developed strategy provided a feasible and operable solution to the bottleneck of the hydrothermal scale-up of $MgBO_2(OH)/Mg_2B_2O_5$ nanowhiskers. Not only was this enlightening for mass production of other nanostructures, especially for the chlorate-participated system in academia and industry, but this also could contribute to sustainable development of our society.

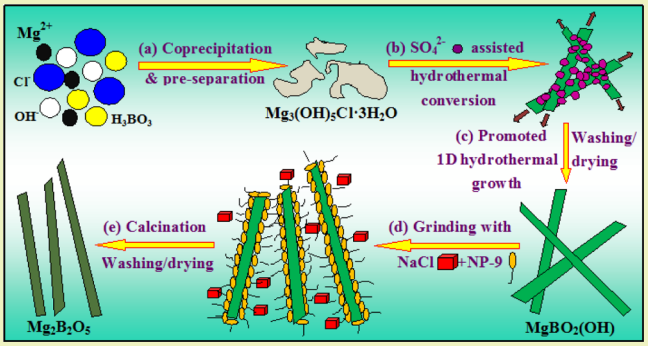

KEYWORDS: *Green, Scale-up, Hydrothermal, Thermal conversion, Magnesium borate, Nanowhiskers*

INTRODUCTION

In the last two decades, one-dimensional (1D) nanomaterials (such as nanotubes, nanowires, nanowhiskers, nanorods, and nanobelts) have attracted much attention for their unique structures, novel properties, and great potential applications in varieties of fields.[1−7] On one hand, the properties of 1D nanomaterials greatly depend on their structures, morphology, aspect ratio and crystallinity,[8−15] and thus, it is of great significance to develop controllable synthetic routes to 1D nanostructures with uniform morphology, high aspect ratio, and high crystallinity. On the other hand, as more and more is recognized in the modern sustainable society, including reducing waste, minimizing energy requirements, conducting synthetic methods at relative lower temperature and pressure, and using renewable raw material or feedstock, significant principles of green chemistry will benefit the sustainable development of our modern society.[16,17] Thus, it is a great challenge to research and develop green synthetic techniques in the materials science and chemical science, as well as the crystalline community.[17]

Conventionally, 1D nanowires or whiskers can be obtained by chemical vapor deposition (CVD),[4,10] molten salt synthesis (MSS),[18] or mechanically activated annealing.[19] For the CVD technique, novel nanostructures with high crystallinity and excellent properties can be obtained. However, problems such as high energy consumption, broad distributions of the size and morphology of products, and difficulty in scaling-up[10] greatly limited its practical utilization at the present stage. As for MSS, high crystallinity whiskers with diameters ranging from several to tens of micrometers can be readily acquired, whereas the relatively large diameters, severe agglomeration, tough post-washing, and purification owing to mass use of NaCl also restrained its development. In contrast, hydrothermal technol-

Received: November 18, 2013
Revised: January 23, 2014
Published: January 27, 2014

ogy has emerged as a thriving method for the synthesis of 1D nanostructures with several distinct advantages, such as energy savings, better nucleation control, better shape control, etc.,[3] which readily leads to hydroxyl- or crystalline water-containing compounds. To obtain anhydrous compounds or oxides, subsequent calcination or thermal conversion is highly considered.

One-dimensional nanostructured magnesium borates, including MgB_4O_7 nanowires,[20] $Mg_3B_2O_6$ nanotubes and nanobelts,[21] $Mg_2B_2O_5$ nanowires,[18,22,23] nanorods[24,25] and whiskers,[26,27] have been paid much attention in recent years for their wide applications as reinforcing components in electronic ceramics,[20] wide band gap semiconductors,[22] glass,[28] and plastics or aluminum/magnesium matrix alloys.[29,30] One-dimensional $Mg_2B_2O_5$ micro/nanostructures were prepared via the traditional high temperature CVD technique[20−23] or MSS route[18,26,27] within 850−1250 °C. As mentioned above, although the $Mg_2B_2O_5$ nanostructures synthesized by the traditional methods exhibited high crystallinity, there were still technical problems needed to be solved, such as high energy consumption, coexistence of the particulate agglomerates,[20,26,27] and relatively rigorous experimental conditions.[21] In our previous work, a hydrothermal-based thermal conversion route has been successfully developed for the $MgBO_2(OH)/Mg_2B_2O_5$ nanowhiskers,[31−34] based on a mass or quasi-pilot hydrothermal production of $MgBO_2(OH)$ nanowhiskers by using an autoclave with a capacity of 150 L that has also been investigated.[35] The temperature and time were 40 °C and 12.0 h lower or shorter than those that had been employed for the optimal hydrothermal synthesis of the $MgBO_2(OH)$ nanowhiskers[36] for fear of the huge corrosive potential of the reactant system containing multitudes of Cl^- to the autoclave. As known, the passivation of chromium oxide can prevent surface corrosion of metals such as steel by blocking oxygen diffusion to the metal surface and further block the corrosion spreading from the surface to the internal structure of the metal. Nevertheless, the electronegative Cl^- ions can inhibit the above-mentioned passivation. The attack of Cl^- toward stainless steel resulted in crevices and pits in the direction perpendicular to the surface being attacked, leading to heavy corrosion of stainless steel. This caused a real decrease in the optimal hydrothermal process to a large extent, producing much shorter $MgBO_2(OH)$ nanowhiskers. The subsequent thermal conversion brought about lower aspect ratio $Mg_2B_2O_5$ nanorods and greatly restrained the corresponding reinforcing effect when filled into the BOPP-D1 type resins.[35] Evidently, the great potential corrosion of the Cl^- ions to the autoclave has emerged as the realistic bottleneck for the hydrothermal scale-up of the nanowhiskers. Thus, to investigate a novel, green, noncorrosive, hydrothermal-based thermal conversion route to $Mg_2B_2O_5$ nanowhiskers has become extremely crucial and imperative for realistic environmentally friendly mass production so as to be employed in related fields in the near future.

In this contribution toward the solution to the significant bottleneck of corrosion originated from the Cl^- ions within the hydrothermal system, we report for the first time our latest results on the green, noncorrosive, easy scale-up, hydrothermal−thermal conversion synthesis of the $Mg_2B_2O_5$ nanowhiskers. In contrast with our previous work,[31−36] the Cl^- ions were avoided to participate in the hydrothermal treatment. SO_4^{2-} were employed to promote 1D growth at lower hydrothermal temperature to acquire high aspect ratio $MgBO_2(OH)$ nanowhiskers. The preseparated filtrate containing NaCl was reused and recycled, and poly(oxyethylene)$_9$ nonylphenol ether (NP-9) was introduced during the thermal conversion so as to produce high aspect ratio, high crystallinity, pore-free $Mg_2B_2O_5$ nanowhiskers with high dispersity. Specifically, the slurry containing NaCl was first filtrated after room-temperature coprecipitation, and the requisite reactant system was then transferred for hydrothermal phase conversion with necessary modulation so as to eliminate the corrosion of Cl^- on the future commercial stainless apparatus. SO_4^{2-}-aided hydrothermal conversion at 200 °C for 12.0 h led to uniform $MgBO_2(OH)$ nanowhiskers (diameter: 10−70 nm, length: 500−3200 nm, aspect ratio: 10−50) with the length and aspect ratio even longer and higher than those previously obtained at 240 °C for 24.0 h.[36] The subsequent thermal conversion in the presence of the byproduct NaCl derived from former filtrate and NP-9 resulted in uniform high crystallinity, high dispersivity, high aspect ratio, pore-free $Mg_2B_2O_5$ nanowhiskers. The present noncorrosive, green, hydrothermal−thermal conversion route to high aspect ratio $MgBO_2(OH)/Mg_2B_2O_5$ nanowhiskers apparently suggested a significant breakthrough based on the previous work, indicating a feasible solution to the future green mass or commercial hydrothermal−thermal conversion production of $MgBO_2(OH)/Mg_2B_2O_5$ nanowhiskers, which is also helpful for green hydrothermal synthesis and mass production of other 1D nanostructured metal oxides with high aspect ratio, high crystallinity, and high dispersity.

EXPERIMENTAL SECTION

Green, Noncorrosive, Easy Scale-Up Hydrothermal Synthesis of $MgBO_2(OH)$ Nanowhiskers. All of the reagents were analytical grade and used directly without further purification. In a typical procedure, the hydrothermal precursor was first prepared by a room-temperature coprecipitation of a $MgCl_2$ (1 mol L^{-1}, 14 mL) solution and H_3BO_3 (0.4996 g) and NaOH (2 mol L^{-1}, 14 mL) solution under vigorous magnetic stirring, keeping the molar ratio of Mg:B:Na as 7:4:14 based on the requisite molar ratio of the reactants at room-temperature coprecipitation.[36] The resultant white slurry was filtered, and the as-obtained cake was washed with deionized (DI) water (resistivity: 1.33×10^5 Ωm) two times (about100 mL in all) in order to remove Cl^-, using a $AgNO_3$ solution to test whether the cake was thoroughly rid of Cl^- or not. The preseparated solution rich in NaCl was saved for reuse. The cake was then put into a Teflon-lined stainless steel autoclave with a capacity of 70 mL by adding 42 mL of DI water. The cake was agitated into a uniform slurry, followed by adding H_3BO_3 with the molar ratio of Mg:additional H_3BO_3 = 7:6.5 (i.e., remanent H_3BO_3 when keeping the total molar ratio of Mg:B = 2:3 according to the previous work[36]), as well as a NaOH solution to adjust the pH value to 10.0−10.2 (i.e., general pH value of the slurry originated from the room-temperature coprecipitation in the previous work). The autoclave was sealed, heated to 200 °C (heating rate: 5 °C min^{-1}), and kept in an isothermal state for 12.0 h. After the hydrothermal synthesis, the autoclave was cooled to room temperature naturally. The as-obtained precipitate was filtered, washed with DI water three times, rinsed with ethanol, and finally dried at 60 °C for 24.0 h for necessary characterization and subsequent thermal conversion. To investigate the possible effect of SO_4^{2-} on the hydrothermal formation of $MgBO_2(OH)$ nanowhiskers, Na_2SO_4 was added into the slurry before the hydrothermal treatment with the molar ratio of $SO_4^{2-}:Mg^{2+}$ = 0.667−0.0125, and other conditions were kept the same.

Thermal Conversion Synthesis of $Mg_2B_2O_5$ Nanowhiskers. For the thermal conversion, the dried hydrothermal product particles were milled in the presence of 61.5% or 100% of the preseparated solution rich in NaCl, 5 mL of NP-9, and 25% or 50% of H_3BO_3 added before the hydrothermal treatment within a quartz mortar for 20.0 min. The resultant slurry was then transferred into a porcelain boat

dx.doi.org/10.1021/sc400481j | ACS Sustainable Chem. Eng. 2014, 2, 836−845

located in a horizontal quartz tube furnace and heated to the designated temperature of 700 °C (heating rate: 1.0−10.0 °C min^{-1}),[34] with the temperature kept constant for 2.0 h. After the thermal conversion, the samples were cooled to room temperature naturally within the tube, collected, washed with DI water three times, and finally dried at 70 °C for 24.0 h.

Characterization. The initial conductivity of the DI water was determined using a conductivity meter (Model DDS-IIA, Shanghai Leici Instrument, Inc., Shanghai, China). The structure of the samples was identified by a X-ray powder diffractometer (XRD, D8-Advance, Bruker, Germany) using Cu Kα radiation (λ = 1.54178 Å) with a fixed power source (40.0 kV, 40.0 mA). The morphologies and structures of the samples were examined by field emission scanning electron microscopy (SEM, JSM, 7401F, JEOL, Japan, at 3.0 kV) and high resolution transmission electron microscopy (TEM, JEM-2010, JEOL, Japan, at 120.0 kV). The selected area electron diffraction (SAED) was also performed by JEM-2010 TEM. The size distribution of the as-synthesized nanowhiskers was estimated by directly measuring about 100 particles from the typical TEM images. The thermal decomposition behavior of the sample was detected by a thermogravimetric analyzer (TGA, Netzsch STA 409C, Germany) carried out in dynamic air with a heating rate of 10.0 K min^{-1}. Pictures of the Tyndall effect were taken by a digital camera, with the nanowhiskers dispersed in the ethanol. Optical properties were examined with a UV−vis spectrophotometer (UV-3600 230VCE, Shimadzu, Japan), with the samples either dispersed in absolute ethanol or simply and directly in the solid state.

RESULTS AND DISCUSSION

Green, Noncorrosive, Easy Scale-Up Hydrothermal Route to $MgBO_2(OH)$ Nanowhiskers. Taking the potential risk of corrosion for the future commercial stainless steel apparatus due to the reactant system rich in NaCl into account, a novel, green, noncorrosive, hydrothermal route to $MgBO_2(OH)$ nanowhiskers was developed and is illustrated in Figure 1. As shown by the red arrow route in the general

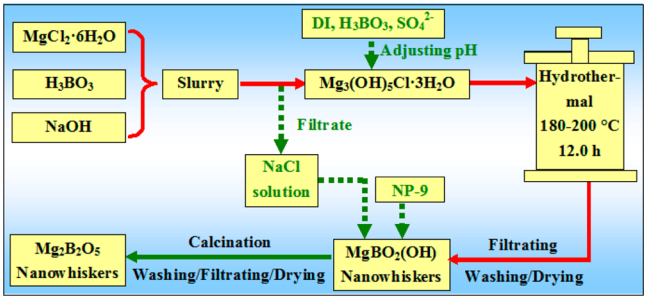

Figure 1. Green, noncorrosive, easy scale-up, hydrothermal−thermal conversion route to high aspect ratio magnesium borate nanowhiskers. Red solid arrow route: Potential corrosive process. Red solid with green dot arrows: Green noncorrosive process.

hydrothermal synthesis, the entire slurry originated from the room-temperature coprecipitation of $MgCl_2$, H_3BO_3, and NaOH solutions (molar ratio of Mg:B:Na as 2:3:4) and was directly transferred into the autoclave for hydrothermal conversion,[36,37] i.e., potential corrosive process. Whereas in the green hydrothermal process (indicated by the red solid and green dot arrows), the slurry derived from the room-temperature coprecipitation (molar ratio of Mg:B:Na = 7:4:14) was filtered, leading to the filtrate rich in NaCl (i.e., NaCl solution) and the cake $Mg_3(OH)_5Cl{\cdot}3H_2O$. The former was set aside for reuse, and the latter was transferred into the autoclave, followed by addition of the requisite reactant H_3BO_3, DI water, SO_4^{2-}, and NaOH to adjust the pH value of the reconstructed phase conversion system to 10.0−10.2. After the hydrothermal phase conversion, the as-obtained product slurry was filtered, washed, and dried, resulting in $MgBO_2(OH)$ nanowhiskers, which were mixed with the NaCl solution and some amount of NP-9 for the subsequent thermal conversion. Finally, byproduct flux NaCl and additional surfactant NP-9 assisted the thermal conversion, giving rise to the final, high crystallinity, pore-free $Mg_2B_2O_5$ nanowhiskers.

Apparently, the hydrothermal−thermal conversion route to $MgBO_2(OH)/Mg_2B_2O_5$ nanowhiskers developed herein was an entirely novel, green, noncorrosive process with easy scale-up. Before the hydrothermal treatment, Cl^- ions within the room-temperature coprecipitation system were preseparated out by filtration and repeated washing, and almost all of the Cl^- ions were transferred into the filtrate. The filtrate rich in Cl^- (in terms of NaCl) was introduced during the thermal conversion procedure and thus could on one hand avoid potential corrosion to the future commercial hydrothermal apparatus. On the other hand, it could serve as the necessary flux medium for pore shrinkage and elimination during the thermal conversion formation of $Mg_2B_2O_5$ nanowhiskers. Within such a conversion, the flux can melt gradually with an increase in temperature and then penetrate into and reach each corner with the generation, coalescence, turbulence, rupture, migration, and evaporation of the pores within the bulk of the porous nanowhiskers due to dehydration and thus promote pore shrinkage and elimination owing to recrystallization.[32,34] Consequently, the byproduct NaCl contained in the preseparated filtrate was recycled and reused. In addition, the hydrothermal conversion was performed below 200 °C for 12.0 h, which was 40 °C lower and 12.0 h shorter than those employed in the previous so-called optimal potential corrosive process,[37,38] indicating significant energy savings. This definitely revealed that the present hydrothermal−thermal conversion route is distinct, novel, green,[39,40] and noncorrosive with an easy scale-up.

It was notable that, however, before the hydrothermal conversion, a necessary amount of DI water, requisite H_3BO_3, and SO_4^{2-} were supplemented to the remnant cake, followed by adding some NaOH solution to adjust the pH value back to that exhibited during the previous potential corrosive hydrothermal process for $MgBO_2(OH)$ nanowhiskers.[31] In addition, the introduction of NP-9 during the thermal conversion of $MgBO_2(OH)$ nanowhiskers was aimed to improve the dispersity of the as-synthesized $Mg_2B_2O_5$ nanowhiskers.

Formation of $MgBO_2(OH)$ Nanowhiskers. To understand the phase conversion throughout the process, both intermediates (i.e., room-temperature coprecipitates or hydrothermal precursors) and the final products were monitored. As shown in Figure 2(a_1), the room-temperature coprecipitates exhibited low crystallinity and were indexed to $Mg_3(OH)_5Cl{\cdot}3H_2O$ (PDF No. 07-0416), which is the same as with the precursor obtained in the previous work when the molar ratio of the reactants were kept as $MgCl_2$:H_3BO_3:NaOH = 2:3:7.[38] The present molar ratio of the reactants (Mg:B:Na = 7:4:14) did not lead to amorphous $Mg_7B_4O_{13}{\cdot}7H_2O$[36] as expected, indicating the requisite boron-rich surrounding for the formation of the $Mg_7B_4O_{13}{\cdot}7H_2O$ phase. In contrast, in the present case, the hydrothermal products formed at 200 °C for 12.0 h whether in the presence of SO_4^{2-} or not (Figure 2(a_2−a_5)) and were all readily assigned to $MgBO_2(OH)$ (PDF No. 39-1370); no other impurities were detected. This was same with that hydrothermally obtained when the molar ratio of the

dx.doi.org/10.1021/sc400481j | ACS Sustainable Chem. Eng. 2014, 2, 836−845

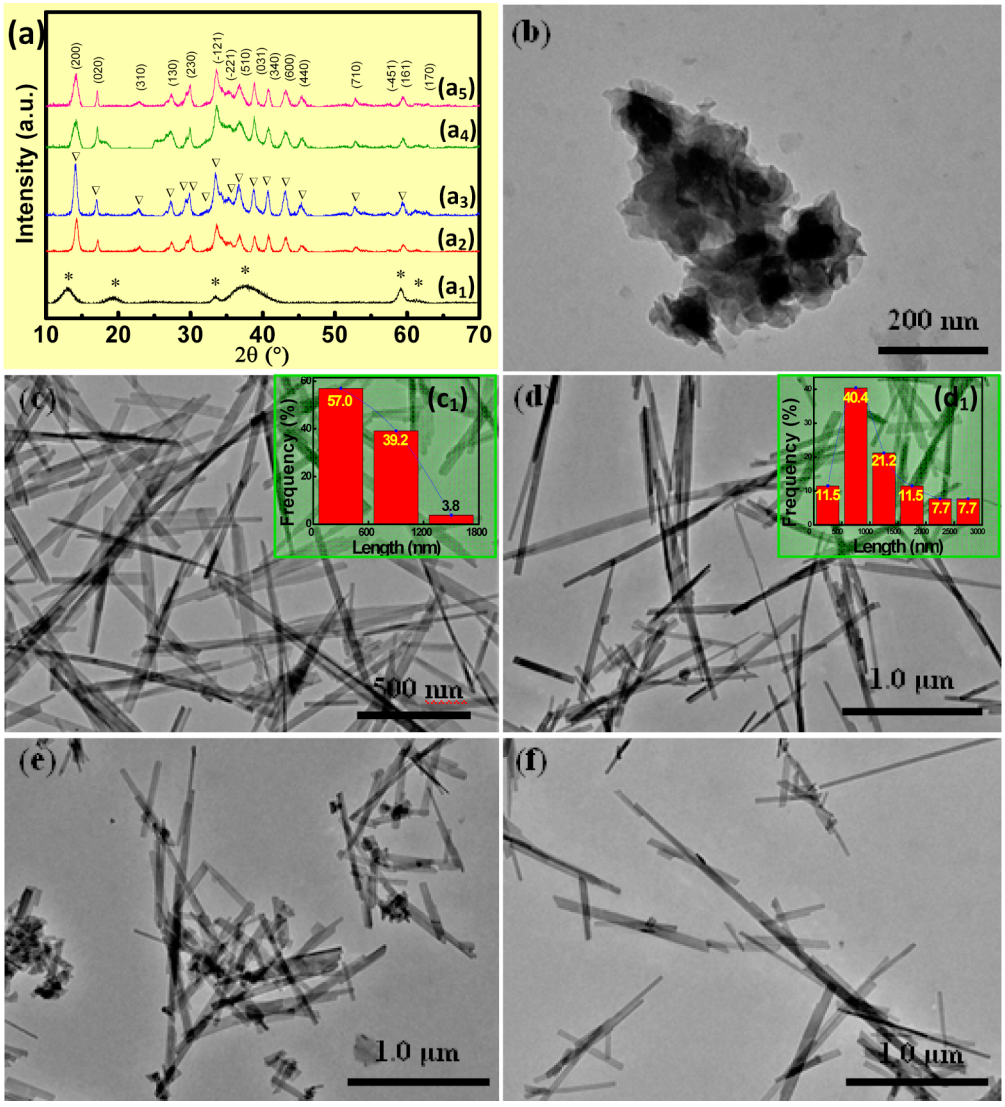

Figure 2. Composition (a_1–a_5) and morphology (b–f) of room-temperature coprecipitation (a_1,b) and hydrothermal products formed at 200 °C for 12.0 h in the absence (a_2,c) or presence (a_3–a_5,d–f) of SO_4^{2-}. Molar ratio of SO_4^{2-}:Mg^{2+} = 0.0125 (a_3,d), 0.05 (a_4,e), and 0.667 (a_5,f). Inserts: Length distribution of the corresponding $MgBO_2(OH)$ nanowhiskers. ∗, $Mg_3(OH)_5Cl{\cdot}3H_2O$; ∇, $MgBO_2(OH)$.

reactants were kept as Mg:B:Na = 2:3:4.[36] Thus, the present room-temperature coprecipitation could be chemically expressed as follows

$$3MgCl_2 + H_3BO_3 + 6NaOH + H_2O \rightarrow Mg_3(OH)_5Cl{\cdot}3H_2O + NaBO_2 + 5NaCl \quad (1)$$

while the supplement of H_3BO_3 and NaOH promoted the hydrothermal conversion from $Mg_3(OH)_5Cl{\cdot}3H_2O$ to $MgBO_2(OH)$

$$Mg_3(OH)_5Cl{\cdot}3H_2O + 3H_3BO_3 + NaOH \rightarrow 3MgBO_2(OH) + NaCl + 9H_2O \quad (2)$$

Meanwhile, the TEM characterization showed that the precursor $Mg_3(OH)_5Cl{\cdot}3H_2O$ exhibited irregular morphology, revealing poor crystallinity (Figure 2b). This was in agreement with the XRD result (Figure 2(a_1)) to some extent. After the hydrothermal treatment, all the $MgBO_2(OH)$ nanoparticles (NPs) demonstrated 1D or whisker-like morphology. As shown in Figure 2 (a_2,c), when hydrothermally treated without any additives, the $MgBO_2(OH)$ nanowhiskers had an average length of 613 nm, a diameter of 34 nm, and an aspect ratio of 18. With the introduction of SO_4^{2-} and the molar ratio of SO_4^{2-}:Mg^{2+} as 0.0125 (a_3,d), the average length and aspect ratio of the $MgBO_2(OH)$ nanowhiskers remarkably increased to 1240 nm and 36, respectively. Detailed size distributions demonstrated that the $MgBO_2(OH)$ nanowhiskers obtained at 200 °C for 12.0 h in the presence of sulfate (Figure S1(a_1–a_3), Supporting Information), molar ratio, SO_4^{2-}:Mg^{2+} = 0.0125) had a length of 0.5–3.0 μm, a diameter of 10–70 nm, and an aspect ratio of 10–80, much longer than those acquired in the absence of sulfate (Figure S1(b_1–b_3), Supporting Information). Notably, the $MgBO_2(OH)$ nanowhiskers synthesized here could be definitely comparable to those acquired at 240 °C for 24.0 h previously[36] in diameter and length, reconfirming the energy savings, green, noncorrosive characteristics of the present hydrothermal route.

In other words, with the molar ratio of SO_4^{2-}: Mg^{2+} increased from 0 to 0.0125, the enhancement effect of the sulfate for the 1D growth of the $MgBO_2(OH)$ nanowhiskers was significant. Although the underlying mechanism is still

dx.doi.org/10.1021/sc400481j | ACS Sustainable Chem. Eng. 2014, 2, 836–845

unclear at present, it was probably associated with the selective adsorption of sulfate on the side surfaces of the $MgBO_2$ (OH) nanowhiskers, which would thus promote the preferential growth of the $MgBO_2(OH)$ nanowhiskers along the axial direction. This was similar to the H_2SO_4-assisted hydrothermal formation of γ-AlOOH nanorods,[41] which exhibited the same 1D growth habit with the $MgBO_2(OH)$ phase owing to the inherent specific anisotropic crystal structure.[37] The inherent anisotropic crystal structure-based 1D growth habit of the nanowhiskers as well as the specific interaction between the sulfate and the side surfaces of the nanowhiskers should have played key roles in enhancing the preferential 1D growth of the $MgBO_2(OH)$ nanowhiskers with longer length and higher aspect ratio.

Nevertheless, when too much sulfate was present, e.g., when the molar ratio of SO_4^{2-}:Mg^{2+} further increased to 0.05 (a_4,e) and to 0.667 (a_5,f), the average length of the nanowhiskers changed to 623 and 900 nm, resepctively, and the average aspect ratio was altered to 15 and 22, respectively. Simultaneously, the average diameter increased to 43 and 42 nm, respectively. Thus, too much sulfate did not further promote the 1D growth of the $MgBO_2(OH)$ nanowhiskers with longer length and larger aspect ratio, and the resultant thicker nanowhiskers in the presence of relatively high sulfate concentration revealed that an excess of sulfate adsorbed onto the side surfaces of the nanowhiskers might favor side coalescence growth, leading to $MgBO_2(OH)$ nanowhiskers with thicker diameters. This was to some extent analogous to the effect of sulfate on the hydrothermal formation of WO_3 nanowires and ribbon-like nanostructures.[42]

The TEM and HRTEM images of the $MgBO_2(OH)$ nanowhiskers formed at 200 °C for 12.0 h in the presence of sulfate (molar ratio of SO_4^{2-}:Mg^{2+} = 0.0125) are shown in Figure 3. As shown, high crystallinity nanowhiskers were

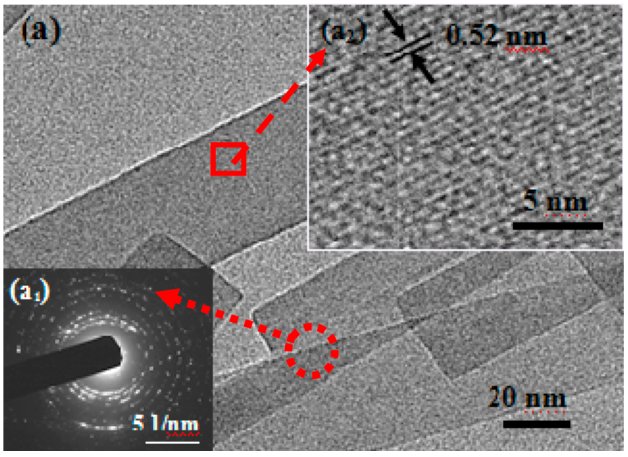

Figure 3. TEM images (a), SAED pattern (a_1), and HRTEM image (a_2) of the $MgBO_2(OH)$ nanowhiskers hydrothermally synthesized at 200 °C for 12.0 h with the molar ratio of SO_4^{2-}:Mg^{2+} = 0.0125.

obtained via the present green noncorrosive hydrothermal route, also comparable to those obtained by the previous hydrothermal process carried out at 240 °C for 24.0 h.[36] The SAED pattern (Figure 3(a_1)) recorded from the dotted circle area indicated that the multilayer nanowhiskers contained within the area were a significant crystalline phase. Meanwhile, the HRTEM image (Figure 3(a_2)) corresponded to the dashed rectangular region demonstrated that the legible longitudinal lattice fringes were observed, and the detected interplanar spacing of 0.52 nm was quite consistent with the standard value of (020) planes, indicating the preferential growth direction of the nanowhiskers parallel to (020) planes, in agreement with the previous results.[38]

Thermal Conversion of $MgBO_2(OH)$ Nanowhiskers To Form $Mg_2B_2O_5$ Nanowhiskers. The thermal decomposition property of the $MgBO_2(OH)$ nanowhiskers synthesized in the presence of SO_4^{2-} (molar ratio, SO_4^{2-}:Mg^{2+}= 0.0125) was examined, as shown in the differential scanning calorimetry (TG-DSC) curves in Figure 4. The mass decreased fast below

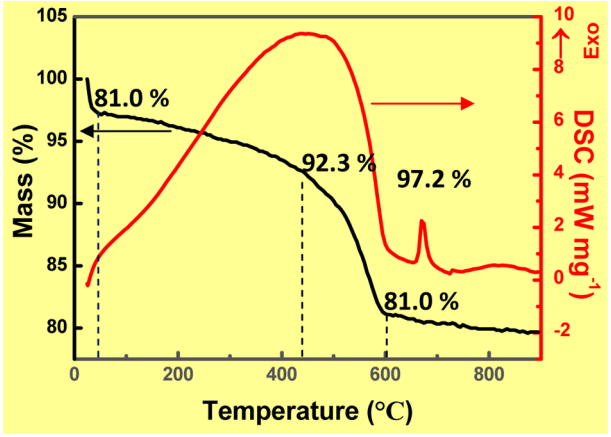

Figure 4. TG-DSC profiles of the $MgBO_2(OH)$ nanowhiskers hydrothermally synthesized at 200 °C for 12.0 h with the molar ratio of SO_4^{2-}:Mg^{2+} = 0.0125.

50 °C, owing to the elimination of the absorbed water derived from the relatively low drying temperature of 60 °C. With the temperature rising, the sample mass decreased at a comparatively slow rate within 50−440 °C and a faster rate within 440−600 °C, which was kept nearly constant at temperature above 600 °C. The mass loss between 440 and 600 °C was 11.3%, similar to the theoretical mass loss (10.7%) for the conversion from $MgBO_2(OH)$ to $Mg_2B_2O_5$

$$2MgBO_2(OH)(s) \rightarrow Mg_2B_2O_5(s) + H_2O(g) \quad (3)$$

As noted previously, the final decomposition temperature of $MgBO_2(OH)$ nanaowhiskers (600 °C) was lower than that of natural szaibelyite ($MgBO_2(OH)$, 700 °C),[43] ascribed to particle size reduction. Simultaneously recorded DSC curves demonstrated that there was a gradual changing tendency below 440 °C and a remarkable endothermic change between 440 and 600 °C, originated from the gradual, steady, however, somewhat difficult elimination of the physically absorbed water and structural water due to the thermal conversion of the $MgBO_2(OH)$ phase (eq 3). The distinct exothermic peak of the DSC curve at approximately 669 °C corresponds to the recrystallization of $Mg_2B_2O_5$.[44] The overal gradual change of the present TG-DSC curves before the final thermal conversion and remarkable exothermic effect after the thermal conversion was quite similar to that demonstrated in previous work[31] and also akin to some other borates.[43,44]

According to the thermal decomposition property of the as-synthesized $MgBO_2(OH)$ nanaowhiskers, subsequent thermal conversion to form $Mg_2B_2O_5$ nanowhiskers was investigated. Because NaCl could be employed as the necessary flux medium for the pore-free $Mg_2B_2O_5$ nanowhiskers,[32] the preseparated

dx.doi.org/10.1021/sc400481j | ACS Sustainable Chem. Eng. 2014, 2, 836−845

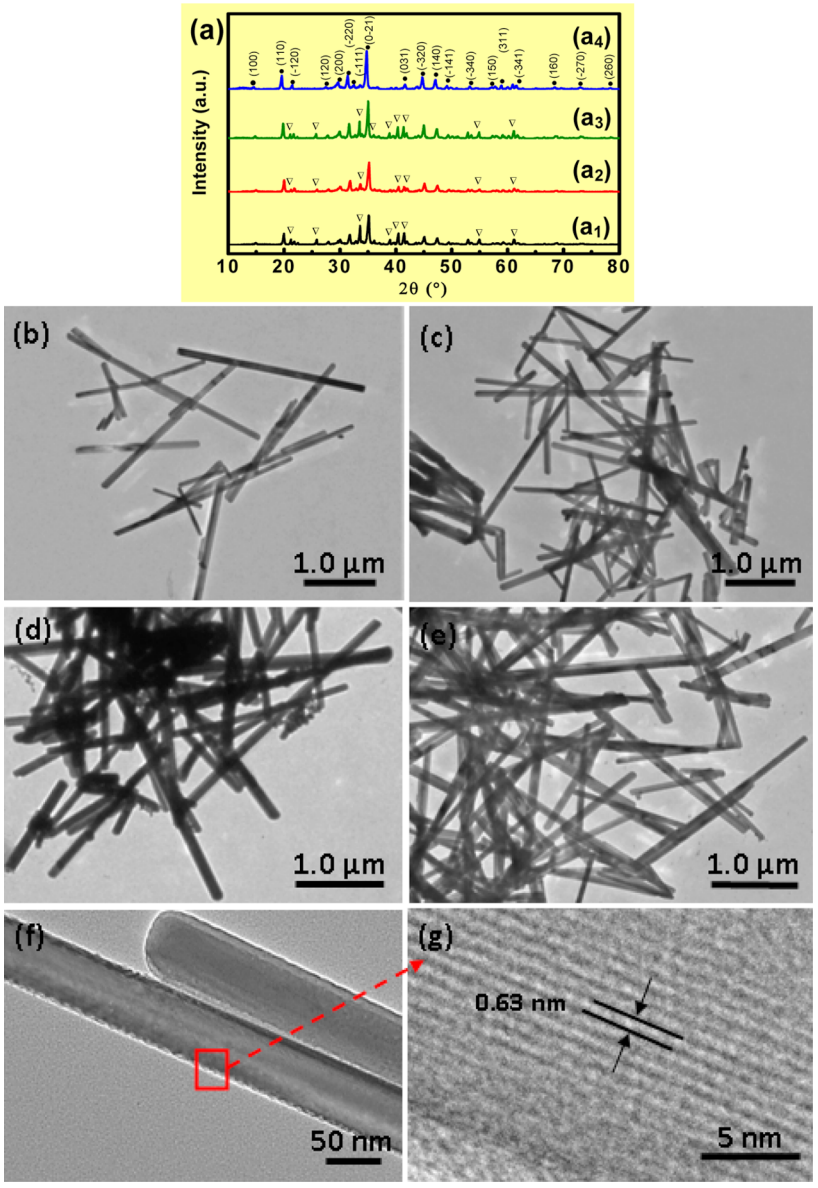

Figure 5. XRD patterns (a_1–a_4), TEM (b–f), and HRTEM (g) images of the products calcined at 700 °C for 2.0 h, assisted by 61.5% (a_1,b) or 100% (a_2,c–g) of the formerly preseparated solution rich in NaCl and NP-9, as well as an additional 25% H_3BO_3 (a_3,d) or 50% H_3BO_3 (a_4,e–g) based on that used before hydrothermal treatment. ●, $Mg_2B_2O_5$; ∇, $Mg_3(BO_3)_2$.

solution rich in NaCl in the present green hydrothermal route could thus be reused. However, in contrast with the previous work,[32] in the preseparated solution rich in NaCl, some amount of additional NP-9 as well as some H_3BO_3 were mixed with the as-obtained $MgBO_2(OH)$ nanaowhiskers before thermal conversion. Figure 5 shows the composition, morphology, and microstructure of the calcined products. When 61.5% of the NaCl-rich solution was used, the calcined product of $Mg_2B_2O_5$ nanowhiskers coexisted remarkably with the $Mg_3(BO_3)_2$ phase (PDF No. 75-1807, Figure 5(a_1,b)). When 100% of the NaCl-rich solution was used, the product was $Mg_2B_2O_5$ nanowhiskers containing less $Mg_3(BO_3)_2$ (Figure 5(a_2,c)). The formation of the impurity phase $Mg_3(BO_3)_2$ should be attributed to the introduction of Mg^{2+} originated from the NaCl-rich solution. To obtain a higher purity calcined product, some necessary H_3BO_3 was introduced before calcination. When 25% of the H_3BO_3 based on that used before the hydrothermal synthesis was added, the product still contained $Mg_3(BO_3)_2$ (Figure 5(a_3,d)). Whenever the amount of H_3BO_3 was further increased to 50% (Figure 5(a_4,e–g)), the calcined products became a uniform pure phase of $Mg_2B_2O_5$ (PDF No. 86-0531) nanowhiskers with a length of 120–3000 nm (Figure S2(a_1), Supporting Information), a diameter of 40–160 nm (Figure S2(a_2), Supporting Information), and an aspect ratio of 2–34 (Figure S2(a_3), Supporting Information). The length, diameter, and aspect ratio of the as-obtained $Mg_2B_2O_5$ nanowhiskers derived from the present green hydrothermal route (200 °C, 12.0 h) could well be comparable to those originated from the traditional hydrothermal synthesis (240 °C, 18.0 h).[32,34,36]

In addition to additional H_3BO_3 and the preseparated slurry rich in NaCl, NP-9 was also employed as the surfactant in the present thermal conversion so as to improve the dispersity of the calcined product, similar to that found in the flux and surfactant-directed facile thermal conversion synthesis of hierarchical porous MgO.[45] As shown in Figure 5(e–g), the

dx.doi.org/10.1021/sc400481j | ACS Sustainable Chem. Eng. 2014, 2, 836–845

as-obtained pore-free $Mg_2B_2O_5$ nanowhiskers were dispersed well, and no significant twin crystals were observed. Thus, the presence of surfactant NP-9 improved the dispersity of the calcined particles on one hand and also constrained the twin crystal formation during the calcination on the other hand. The HRTEM image (Figure 5 (g)) recorded from the red rectangular region of the typical $Mg_2B_2O_5$ nanowhisker in Figure 5 (f) reconfirmed the high crystallinity of the product. The detected interplanar spacing of 0.63 nm corresponding to the legible longitudinal lattice fringes was quite similar to the standard value of (100) planes (0.60 nm), indicating the preferential growth of the $Mg_2B_2O_5$ nanowhisker parallel to (100) planes. This was in agreement with the preferential growth along the [010] direction of those acquired by the traditional hydrothermal-based thermal conversion.[32]

Green Hydrothermal−Thermal Conversion Formation Mechanism of $Mg_2B_2O_5$ Nanowhiskers. Apparently, preseparation of Cl^- and introduction of SO_4^{2-}, NaCl, and NP-9 played significant roles on the formation of the high aspect ratio, high crystallinity, and high dispersivity $MgBO_2(OH)/Mg_2B_2O_5$ nanowhiskers; the overall green hydrothermal−thermal conversion formation mechanism is depicted in Figure 6. As shown, the sulfate and surfactant-directed green hydrothermal−thermal conversion formation consisted of several stages. First, the room-temperature coprecipitation of $MgCl_2$, H_3BO_3 ,and NaOH solutions and preseparation of Cl^- led to low crystallinity $Mg_3(OH)_5Cl{\cdot}3H_2O$ with irregular morphology. Second, during the hydrothermal phase conversion, the selective adsorption of SO_4^{2-} onto specific side surfaces of the originally formed 1D subunits restrained the side growth to some extent. Third, the selective adsorption of SO_4^{2-} and continuous hydrothermal treatment (200 °C, 12.0 h) promoted the preferential 1D growth along the axial direction, resulting in high aspect ratio $MgBO_2(OH)$ nanowhiskers. Fourth, the grinding of the $MgBO_2(OH)$ nanowhiskers and the surfactant NP-9 as well as preseparated filtrate containing NaCl gave rise to the slurry containing byproduct NaCl and NP-9 wrapped $MgBO_2(OH)$ nanowhiskers. Finally, the calcination of the formerly mixed slurry (700 °C, 2.0 h) and ultimate washing and drying produced high aspect ratio pore-free $Mg_2B_2O_5$ nanowhiskers with good dispersity.

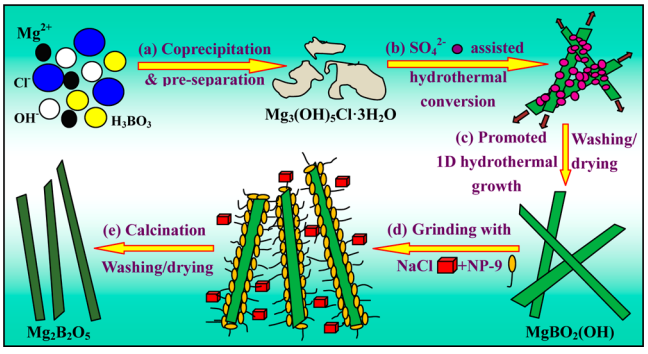

Figure 6. Sulfate and surfactant-directed green hydrothermal−thermal conversion formation of high aspect ratio, high dispersivity, pore-free $Mg_2B_2O_5$ nanowhiskers. (a) Room-temperature coprecipitation of $MgCl_2$, H_3BO_3, and NaOH solutions and preseparation of Cl^- led to low crystallinity $Mg_3(OH)_5Cl{\cdot}3H_2O$ with irregular morphology. (b) During the hydrothermal phase conversion, selective adsorption of SO_4^{2-} onto specific side surfaces of the originally formed 1D subunits restrained the side growth to some extent. (c) Selective adsorption of SO_4^{2-} and continuous hydrothermal treatment (200 °C, 12.0 h) promoted the preferential 1D growth along the axial direction, resulting in high aspect ratio $MgBO_2(OH)$ nanowhiskers. (d) Grinding the $MgBO_2(OH)$ nanowhiskers with the surfactant NP-9 and preseparated filtrate containing NaCl gave rise to the slurry containing byproduct NaCl and NP-9 wrapped $MgBO_2(OH)$ nanowhiskers. (e) Calcination of the formerly mixed slurry (700 °C, 2.0 h) and final washing and drying produced high aspect ratio pore-free $Mg_2B_2O_5$ nanowhiskers with good dispersity.

Tyndall Effects and Optical Absorbance Properties of $MgBO_2(OH)$ and $Mg_2B_2O_5$ Nanowhiskers. Dispersive stability of the $MgBO_2(OH)$ and $Mg_2B_2O_5$ nanowhiskers was evaluated via the Tyndall effect, as shown in Figure 7. When dispersed in ethanol for hydrothermal treatment and kept standing for 15 min, both solvents containing $MgBO_2(OH)$ nanowhiskers (Figure 7(a_1)) and $Mg_2B_2O_5$ nanowhiskers (Figure 7(a_2)) demonstrated a typical Tyndall effects, as illuminated by a red laser indicator. The straight and narrow light path indicated the as-prepared systems were of colloidal characteristic with fine nanowhiskers with relatively uniform size distribution and also good dispersion. In contrast, both systems became a little turbid after standing for 10 days, and the Tyndall effects were also obvious with the light paths slightly dispersed at the ends (Figure 7(b_1,b_2)). The Tyndall effects revealed the good dispersion and satisfactory stability of the present $MgBO_2(OH)$ and $Mg_2B_2O_5$ nanowhiskers within ethanol, which further suggested potential good compatibility when the as-obtained nanowhiskers are employed in the future as enforcements for polymers such as resins, plastics, rubbers, and so on.

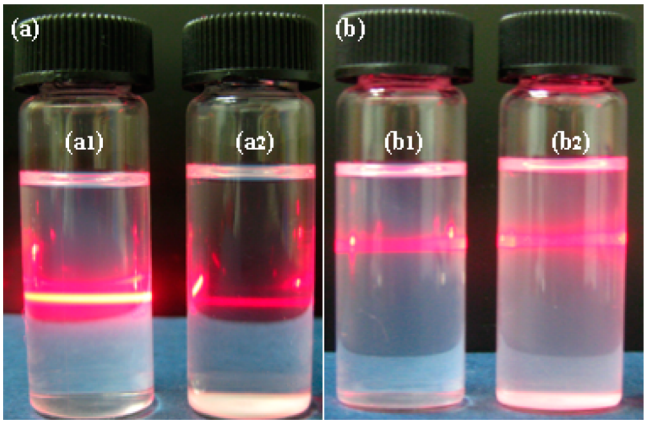

Figure 7. Tyndall effect of the $MgBO_2(OH)$ nanowhiskers (a_1,b_1) hydrothermally synthesized at 200 °C for 12.0 h with the molar ratio of SO_4^{2-}:Mg^{2+} = 0.0125 and corresponding $Mg_2B_2O_5$ nanowhiskers (a_2,b_2) calcined at 700 °C for 2.0 h in the presence of 100% of the preseparated solution rich in NaCl and an additional 50% H_3BO_3 and NP-9, both of which were dispersed in ethanol for ultrasonical treatment and then were kept standing for 15 min (a_1,a_2) or 10 days (b_1,b_2).

Figure 8 shows the UV−vis spectra of the $MgBO_2(OH)$ nanowhiskers (a_1,b_1) and corresponding $Mg_2B_2O_5$ nanowhiskers (a_2,b_2) dispersed in ethanol (a_1,a_2) or directly in the solid state (b_1,b_2). When dispersed in ethanol, $MgBO_2(OH)$ nanowhiskers did not demonstrate distinct absorption within the whole wavelength range (300−900 nm), revealing good transparency from the near-ultraviolet to near-infrared region. This was quite similar to the transparent characteristic of the $Ba_3B_6O_9(OH)_6$ nanorods and β-BaB_2O_4 nanospindles,[46] also

dx.doi.org/10.1021/sc400481j | ACS Sustainable Chem. Eng. 2014, 2, 836−845

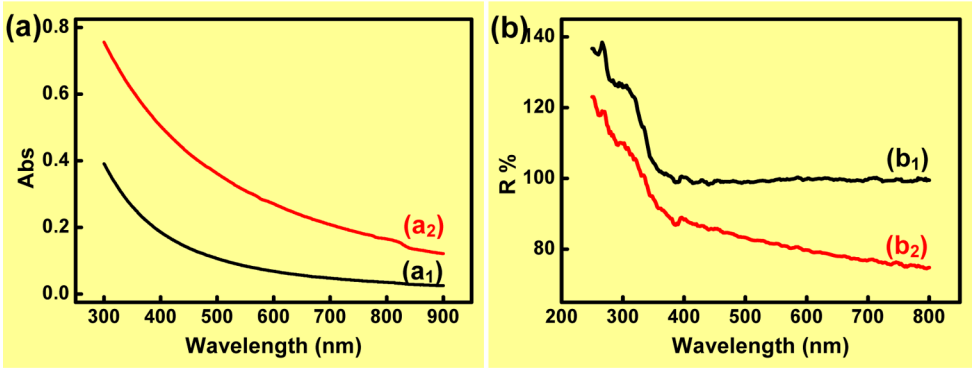

Figure 8. UV−vis spectra of the $MgBO_2(OH)$ nanowhiskers (a_1,b_1) hydrothermally synthesized at 200 °C for 12.0 h with the molar ratio of SO_4^{2-}:Mg^{2+} = 0.0125,and corresponding $Mg_2B_2O_5$ nanowhiskers calcined at 700 °C for 2.0 h in the presence of 100% of the preseparated solution rich in NaCl and an additional 50% H_3BO_3 and NP-9 (a_2,b_2), both of which were dispersed in ethanol (a_1,a_2) or directly in the solid state (b_1,b_2).

analogous to the $Ca_2B_2O_5{\cdot}H_2O/Ca_2B_2O_5$ nanobelts.[47] In contrast, $Mg_2B_2O_5$ nanowhiskers exhibited a weak absorption within the near-infrared region of 800−850 nm. When measured directly in the solid state, both $MgBO_2(OH)$ nanowhiskers and $Mg_2B_2O_5$ nanowhiskers demonstrated weak absorption within the near-ultraviolet region (260−350 nm) as well as the visible light range (400−450 nm).

CONCLUSIONS

The uniform and pore-free $Mg_2B_2O_5$ nanowhiskers (length: 120−3000 nm, diameter: 40−160 nm, aspect ratio: 2−34) were successfully synthesized via a novel, green, noncorrosive, easy scale-up hydrothermal (200 °C, 12.0 h) route-based thermal conversion (700 °C, 2.0 h), using $MgCl_2$, H_3BO_3, and NaOH as the raw materials. Specifically, the room-temperature coprecipitation of the reactants led to low crystallinity $Mg_3(OH)_5Cl{\cdot}3H_2O$ first, which was transferred for hydrothermal conversion after a preseparation of the filtrate rich in NaCl to avoid corrosion of Cl^-, and then some necessary amounts of H_3BO_3, NaOH, and Na_2SO_4 were added, resulting in uniform $MgBO_2(OH)$ nanowhiskers (length: 500−3000 nm, diameter: 10−70 nm, aspect ratio: 10−80). The as-obtained $MgBO_2(OH)$ nanowhiskers were subsequently calcined to further form high crystallinity $Mg_2B_2O_5$ nanowhiskers, assisted by NP-9 as well as byproduct NaCl, which was derived from the preseparated filtrate. The present novel hydrothermal synthetic route to $MgBO_2(OH)$ nanowhiskers was performed at distinctly mild conditions, 40 °C lower than previous work. Most importantly, the as-obtained nanowhiskers could be comparable to those synthesized by the previous high-temperature hydrothermal process in terms of length and aspect ratio. This definitely indicated that the present synthetic route to $MgBO_2(OH)/Mg_2B_2O_5$ nanowhiskers had green characteristics, such as energy savings, no need of additional abundant flux, reduction and reuse of byproducts (filtrate rich in NaCl), noncorrosiveness to the hydrothermal apparatus, and easy commercial scale-up. The introduction of trace amounts of Na_2SO_4 and NP-9 was for promoting the 1D preferential hydrothermal growth of $MgBO_2(OH)$ nanowhiskers and improving the dispersion of the calcined $Mg_2B_2O_5$ nanowhiskers, respectively. The as-developed strategy was believed to be a feasible and an operable solution to the bottleneck of the scale-up and future commercialization of the hydrothermal−thermal conversion process for the high crystallinity and high aspect ratio $MgBO_2(OH)/Mg_2B_2O_5$ nanowhiskers, which was not only enlightening for hydrothermal scale-up of other nanostructures, especially the chlorate-participated system in academia and industry, but also could contribute to sustainable development.

ASSOCIATED CONTENT

Supporting Information

Size distribution of the $MgBO_2(OH)$ nanowhiskers hydrothermally synthesized at 200 °C for 12.0 h in the presence or absence of sulfate (Figure S1) and size distribution of the corresponding $Mg_2B_2O_5$ nanowhiskers calcined at 700 °C for 2.0 h in the presence of 100% of the preseparated solution rich in NaCl, additional 50% H_3BO_3, and NP-9 (Figure S2). This material is available free of charge via the Internet at http://pubs.acs.org.

AUTHOR INFORMATION

Corresponding Authors

*Tel.:+86-537-4453130. E-mail: zhuwancheng@tsinghua.org.cn (W.Z.).

*Fax:+86-10-6277-2051. E-mail: zhang-qiang@mails.tsinghua.edu.cn (Q.Z.).

Notes

The authors declare no competing financial interest.

ACKNOWLEDGMENTS

This work was supported by the National Natural Science Foundation of China (No. 21276141), and the State Key Laboratory of Chemical Engineering, China (No. SKL-ChE-12A05). The authors thank Dr. Yuanyuan Feng and Dr. Xiao Zhu at the School of Chemistry and Chemical Engineering, Qufu Normal University, for their helpful discussion and assistance in the measurement of resistivity of DI water. We also are obliged to the reviewers for their constructive suggestions.

REFERENCES

(1) Xia, Y. N.; Yang, P. D.; Sun, Y. G.; Wu, Y. Y.; Mayers, B.; Gates, B.; Yin, Y. D.; Kim, F.; Yan, Y. Q. One-dimensional nanostructures: Synthesis, characterization, and applications. *Adv. Mater.* **2003**, *15*, 353−389.

(2) Li, J.; Lin, J.; Xu, X.; Zhang, X.; Xue, Y.; Mi, J.; Mo, Z.; Fan, Y.; Hu, L.; Yang, X.; Zhang, J.; Meng, F.; Yuan, S.; Tang, C. Porous boron nitride with a high surface area: Hydrogen storage and water treatment. *Nanotechnology* **2013**, *24*, 155603−155609.

(3) Wang, X.; Zhuang, J.; Chen, J.; Zhou, K.; Li, Y. Thermally stable silicate nanotubes. *Angew. Chem., Int. Ed.* **2004**, *43*, 2017−2020.

(4) See, C. H.; Harris, A. T. A review of carbon nanotube synthesis *via* fluidized-bed chemical vapor deposition. *Ind. Eng. Chem. Res.* **2007**, *46*, 997−1012.
(5) Li, S.; Xu, D.; Shen, H.; Zhou, J.; Fan, Y. Synthesis and Raman properties of magnesium borate micro/nanorods. *Mater. Res. Bull.* **2012**, *47*, 3650−3653.
(6) Shi, W.; Song, S.; Zhang, H. Hydrothermal synthetic strategies of inorganic semiconducting nanostructures. *Chem. Soc. Rev.* **2013**, *42*, 5714−5743.
(7) Zhang, Q.; Huang, J.-Q.; Qian, W.-Z.; Zhang, Y.-Y.; Wei, F. The road for nanomaterials industry: A review of carbon nanotube production, post-treatment, and bulk applications for composites and energy storage. *Small* **2013**, *9*, 1237−1265.
(8) Sun, X.; Xiang, L. Hydrothermal conversion of magnesium oxysulfate whiskers to magnesium hydroxide nanobelts. *Mater. Chem. Phys.* **2008**, *109*, 381−385.
(9) Chen, J.; Xiang, L. Controllable synthesis of calcium carbonate polymorphs at different temperatures. *Powder Technol.* **2009**, *189*, 64−69.
(10) Zhang, Q.; Huang, J.-Q.; Zhao, M.-Q.; Qian, W.-Z.; Wei, F. Carbon nanotube mass production: Principles and processes. *ChemSusChem* **2011**, *4*, 864−889.
(11) Li, R.; Bao, L.; Li, X. Synthesis, structural, optical and mechanical characterization of SrB_2O_4 nanorods. *CrystEngComm* **2011**, *13*, 5858−5862.
(12) Zhu, W. C.; Yang, Y.; Hu, S.; Xiang, G.; Xu, B.; Zhuang, J.; Wang, X. $(Ni,Mg)_3Si_2O_5(OH)_4$ Solid-solution nanotubes supported by Sub-0.06 wt % palladium as a robust high-efficiency catalyst for Suzuki−Miyaura cross-coupling reactions. *Inorg. Chem.* **2012**, *51*, 6020−6031.
(13) Zhao, M.-Q.; Zhang, Q.; Huang, J.-Q.; Wei, F. Hierarchical nanocomposites derived from nanocarbons and layered double hydroxides: Properties, synthesis, and applications. *Adv. Funct. Mater.* **2012**, *22*, 675−694.
(14) Wang, P.; Ma, J.; Shi, F.; Ma, Y.; Wang, Z.; Zhao, X. Behaviors and effects of differing dimensional nanomaterials in water filtration membranes through the classical phase inversion process: A review. *Ind. Eng. Chem. Res.* **2013**, *52*, 10355−10363.
(15) Wang, D. W.; Zeng, Q. C.; Zhou, G. M.; Yin, L. C.; Li, F.; Cheng, H. M.; Gentle, I. R.; Lu, G. Q. M. Carbon-sulfur composites for Li-S batteries: Status and prospects. *J. Mater. Chem. A* **2013**, *1*, 9382−9394.
(16) Veeramani, H.; Aruguete, D.; Monsegue, N.; Murayama, M.; Dippon, U.; Kappler, A.; Hochella, M. F. Low-temperature green synthesis of multivalent manganese oxide nanowires. *ACS Sustainable Chem. Eng.* **2013**, *1*, 1070−1074.
(17) Bergeson, L. L. Sustainable nanomaterials: Emerging governance systems. *ACS Sustainable Chem. Eng.* **2013**, *1*, 724−730.
(18) Tao, X. Y.; Li, X. D. Catalyst-free synthesis, structural, and mechanical characterization of twinned $Mg_2B_2O_5$ nanowires. *Nano Lett.* **2008**, *8*, 505−510.
(19) Ağaoğullari, D.; Balci, Ö.; Gökçe, H.; Duman, İ.; Öveçoğlu, M. L. Synthesis of magnesium borates by mechanically activated annealing. *Metallurgical and Materials Transactions A* **2012**, *43*, 2520−2533.
(20) Ma, R. Z.; Bando, Y.; Sato, T. Nanowires of metal borates. *Appl. Phys. Lett.* **2002**, *81*, 3467−3469.
(21) Ma, R. Z.; Bando, Y.; Golberg, D.; Sato, T. Nanotubes of magnesium borate. *Angew. Chem., Int. Ed.* **2003**, *115*, 1880−1882.
(22) Li, Y.; Fan, Z. Y.; Lu, J. G.; Chang, R. P. H. Synthesis of magnesium borate ($Mg_2B_2O_5$) nanowires by chemical vapor deposition method. *Chem. Mater.* **2004**, *16*, 2512−2514.
(23) Zeng, Y.; Yang, H. B.; Fu, W. Y.; Qiao, L.; Chang, L. X.; Chen, J. J.; Zhu, H. Y.; Li, M. H.; Zou, G. T. Synthesis of magnesium borate ($Mg_2B_2O_5$) nanowires, growth mechanism and their lubricating properties. *Mater. Res. Bull.* **2008**, *43*, 2239−2247.
(24) Elssfah, E. M.; Elsanousi, A.; Zhang, J.; Song, H. S.; Tang, C. C. Synthesis of magnesium borate nanorods. *Mater. Lett.* **2007**, *61*, 4358−4361.
(25) Xu, B.; Li, T.; Zhang, Y.; Zhang, Z.; Liu, X.; Zhao, J. New synthetic route and characterization of magnesium borate nanorods. *Cryst. Growth Des.* **2008**, *8*, 1218−1222.
(26) Sakane, K.; Kitamura, T.; Wada, H.; Suzue, M. Effect of mixing state of raw materials in the preparation of $Mg_2B_2O_5$ whiskers. *Adv. Powder Technol.* **1992**, *3*, 39−46.
(27) Kitamura, T.; Sakane, K.; Wada, H. Formation of needle crystals of magnesium pyroborate. *J. Mater. Sci. Lett.* **1988**, *7*, 467−469.
(28) Dou, L. S.; Zhong, J. C.; Wang, H. Z. Preparation and characterization of magnesium borate for special glass. *Phys. Scr.* **2010**, *2010*, 014010.
(29) Chen, S. H.; Jin, P. P.; Schumacher, G.; Wanderka, N. Microstructure and interface characterization of a cast $Mg_2B_2O_5$ whisker reinforced AZ91D magnesium alloy composite. *Compos. Sci. Technol.* **2010**, *70*, 123−129.
(30) Li, J.; Wang, F.; Weng, W.; Zhang, Y.; Wang, M.; Wang, H. Characteristic and mechanical properties of magnesium matrix composites reinforced with $Mg_2B_2O_5$w and B_4Cp. *Mater. Design.* **2012**, *37*, 533−536.
(31) Zhu, W. C.; Xiang, L.; Zhang, Q.; Zhang, X. Y.; Hu, L.; Zhu, S. L. Morphology preservation and crystallinity improvement in the thermal conversion of the hydrothermal synthesized $MgBO_2(OH)$ nanowhiskers to $Mg_2B_2O_5$ nanowhiskers. *J. Cryst. Growth* **2008**, *310*, 4262−4267.
(32) Zhu, W. C.; Zhang, Q.; Xiang, L.; Wei, F.; Sun, X. T.; Piao, X. L.; Zhu, S. L. Flux-assisted thermal conversion route to pore-free high crystallinity magnesium borate nanowhiskers at a relatively low temperature. *Cryst. Growth Des.* **2008**, *8*, 2938−2945.
(33) Zhu, W. C.; Zhang, Q.; Xiang, L.; Zhu, S. L. Green co-precipitation byproduct-assisted thermal conversion route to sub-micron $Mg_2B_2O_5$ whiskers. *CrystEngComm* **2011**, *13*, 1654−1663.
(34) Zhu, W. C.; Zhang, Q.; Xiang, L.; Zhu, S. L. Repair the pores and preserve the morphology: Formation of high crystallinity 1D nanostructures via the thermal conversion route. *Cryst. Growth Des.* **2011**, *11*, 709−718.
(35) Zhu, W. C.; Li, G. D.; Zhang, Q.; Xiang, L.; Zhu, S. L. Hydrothermal mass production of $MgBO_2(OH)$ nanowhiskers and subsequent thermal conversion to $Mg_2B_2O_5$ nanorods for biaxially oriented polypropylene resins reinforcement. *Powder Technol.* **2010**, *203*, 265−271.
(36) Zhu, W. C.; Xiang, L.; He, T. B.; Zhu, S. L. Hydrothermal synthesis and characterization of magnesium borate hydroxide nanowhiskers. *Chem. Lett.* **2006**, *35*, 1158−1159.
(37) Zhu, W. C.; Zhu, S. L.; Xiang, L. Successive effect of rolling up, oriented attachment and Ostwald ripening on the hydrothermal formation of szaibelyite $MgBO_2(OH)$ nanowhiskers. *CrystEngComm* **2009**, *11*, 1910−1919.
(38) Zhu, W. C.; Xiang, L.; Zhang, X.; Zhu, S. Influence of process parameters on hydrothermal formation of magnesium borate hydroxide nanowhiskers. *Mater. Res. Innov.* **2007**, *11*, 188−192.
(39) Jenck, J. F.; Agterberg, F.; Droescher, M. J. Products and processes for a sustainable chemical industry: A review of achievements and prospects. *Green Chem.* **2004**, *6*, 544−556.
(40) Anastas, P.; Eghbali, N. Green chemistry: Principles and practice. *Chem. Soc. Rev.* **2010**, *39*, 301−312.
(41) He, T. B.; Xiang, L.; Zhu, W. C.; Zhu, S. L. H_2SO_4-assisted hydrothermal preparation of γ-AlOOH nanorods. *Mater. Lett.* **2008**, *62*, 2939−2942.
(42) Gu, Z. J.; Zhai, T. Y.; Gao, B. F.; Sheng, X. H.; Wang, Y. B.; Fu, H. B.; Ma, Y.; Yao, J. N. Controllable Assembly of WO_3 Nanorods/Nanowires into Hierarchical Nanostructures. *J. Phys. Chem. B* **2006**, *110*, 23829−23836.
(43) Xie, X. D.; Zheng, M. P.; Liu, L. B. *Borates Minerals*; Science Press: Beijing, 1965; pp 54−57.
(44) Zhihong, L.; Mancheng, H.; Shiyang, G. Studies on Synthesis, Characterization and Thermochemistry of $Mg_2[B_2O_4(OH)_2]\cdot H_2O$. *J. Therm. Anal. Calorim* **2004**, *75*, 73−78.
(45) Zhu, W. C.; Zhang, L.; Tian, G.-L.; Wang, R.; Zhang, H.; Piao, X.; Zhang, Q. Flux and surfactant directed facile thermal conversion

synthesis of hierarchical porous MgO for efficient adsorption and catalytic growth of carbon nanotubes. *CrystEngComm* **2014**, *16*, 308−318.
(46) Li, R.; Tao, X. Y.; Li, X. D. Low temperature, organic-free synthesis of $Ba_3B_6O_9(OH)_6$ nanorods and Beta-BaB_2O_4 nanospindles. *J. Mater. Chem.* **2009**, *19*, 983−987.
(47) Zhu, W. C.; Zhang, X.; Wang, X. L.; Zhang, H.; Zhang, Q.; Xiang, L. Short belt-like $Ca_2B_2O_5{\cdot}H_2O$ nanostructures: Hydrothermal formation, FT-IR, thermal decomposition, and optical properties. *J. Cryst. Growth* **2011**, *332*, 81−86.